Journal of Medicinal Chemistry

Article

pubs.acs.org/jmc

Bicyclization and Tethering to Albumin Yields Long-Acting Peptide Antagonists

Alessandro Angelini,[†] Julia Morales-Sanfrutos,[‡] Philippe Diderich, Shiyu Chen, and Christian Heinis*

Institute of Chemical Sciences and Engineering, Ecole Polytechnique Fédérale de Lausanne, CH-1015 Lausanne, Switzerland

Supporting Information

ABSTRACT: Proteolytically stable peptide architectures are required for the development of long-acting peptide therapeutics. In this work, we found that a phage-selected bicyclic peptide antagonist exhibits an unusually high stability in vivo and subsequently deciphered the underlying mechanisms of peptide stabilization. We found that the bicyclic peptide was significantly more stable than its constituent rings synthesized as two individual macrocycles. The two rings protect each other from proteolysis when linked together, conceivably by constraining the conformation and/or by mutually shielding regions prone to proteolysis. A second stabilization mechanism was found when the bicyclic peptide was linked to an albumin-binding peptide to prevent its rapid renal clearance. The bicyclic peptide conjugate not only circulated 50-fold longer ($t_{1/2}$ = 24 h) but also became entirely resistant to proteolysis when tethered to the long-lived serum protein. The bicyclic peptide format overcomes a limitation faced by many peptide leads and appears to be suitable for the generation of long-acting peptide therapeutics.

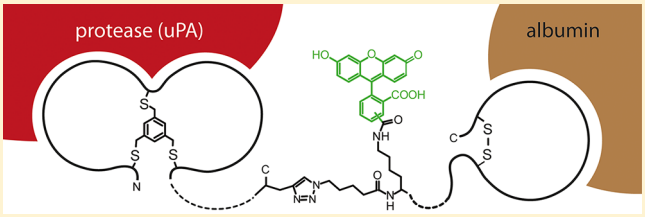

INTRODUCTION

Peptides possess a number of potential benefits as therapeutics, including high potency and target specificity as well as low toxicity. At the same time, they have limiting properties such as their generally low metabolic stability and rapid renal clearance. During systemic circulation, most peptides are degraded within minutes by peptidases in the blood, liver, and kidney.[1] Peptides that are not degraded by proteases are nevertheless rapidly eliminated by glomerular filtration in the kidney, typically with half-lives of less than an hour. In recent years, a number of strategies have been developed to counteract this latter mechanism of peptide elimination.[2,3] These strategies, including linkage of the peptides to large polymers (e.g., PEG) or fusion to long-lived serum proteins such as albumin or the Fc antibody fragment of IgG, have extended peptide elimination half-lives to the order of days. To benefit from such prolonged circulation times, the peptides need to be proteolytically stable to exert their activity throughout their time in circulation. This is exemplified by a recent work in which the monocyclic natriuretic peptide was linked to an antibody Fc fragment but could not fully benefit from the long circulation time of the Fc ($t_{1/2}$ of around 2 days in mice) because the peptide was proteolytically degraded.[4] The requirement for higher metabolic stability should therefore be taken into account in the development of peptide agonists or antagonists designed to circulate for an extended time in the body.

Proteolytic stability depends mainly on the amino acid sequence and peptide format. While linear peptides are typically degraded within minutes in systemic circulation, cyclic structures tend to be more stable. This is because the peptide ends of cyclic structures are not accessible to exopeptidases and the backbones of cyclized peptides are less flexible, preventing an optimal fit to the active sites of endopeptidases.[5] In fact, many natural peptides are cyclic[6] and have presumably evolved to confer binding and stability advantages over their ancestral linear peptides. Examples are the peptide hormones oxytocin, somatostatin, and atrial natriuretic peptide, which have longer half-lives than their linear counterparts.[7−9] Stabilization through cyclization is even more pronounced for multicyclic peptides. Many natural peptides and small proteins are cyclized by two or more disulfide bridges and show enhanced stability due to a significantly reduced sensitivity to proteolytic cleavage. One remarkable family of multicyclic peptides, the cystine knot proteins, contains three disulfide bridges organized in a knotted structure.[10] An example is conotoxin ω-MVIIA, a cystine knot isolated from marine cone snail venom, which is clinically used for its analgesic activity.[11] In cyclotides, a subfamily of cystine knot proteins, the backbone is additionally cyclized head-to-tail, enhancing topological complexity and stability. The prototype of this subfamily, kalata B1, was not digested even after incubation with high protease concentrations.[12] Cyclic peptides enriched for biological activities and evolved for higher stability have been extracted from diverse natural sources. For example, a library rich in multicyclic peptides (termed Melusine) was generated by fractionation of more than 1200 animal venoms and is provided by Atheris/Bachem.[13]

De novo-generated peptide ligands are typically developed based on cyclic structures to exploit their inherently higher stability. Large random libraries of disulfide-cyclized peptides

Received: September 5, 2012
Published: October 22, 2012

dx.doi.org/10.1021/jm301276e | J. Med. Chem. 2012, 55, 10187−10197

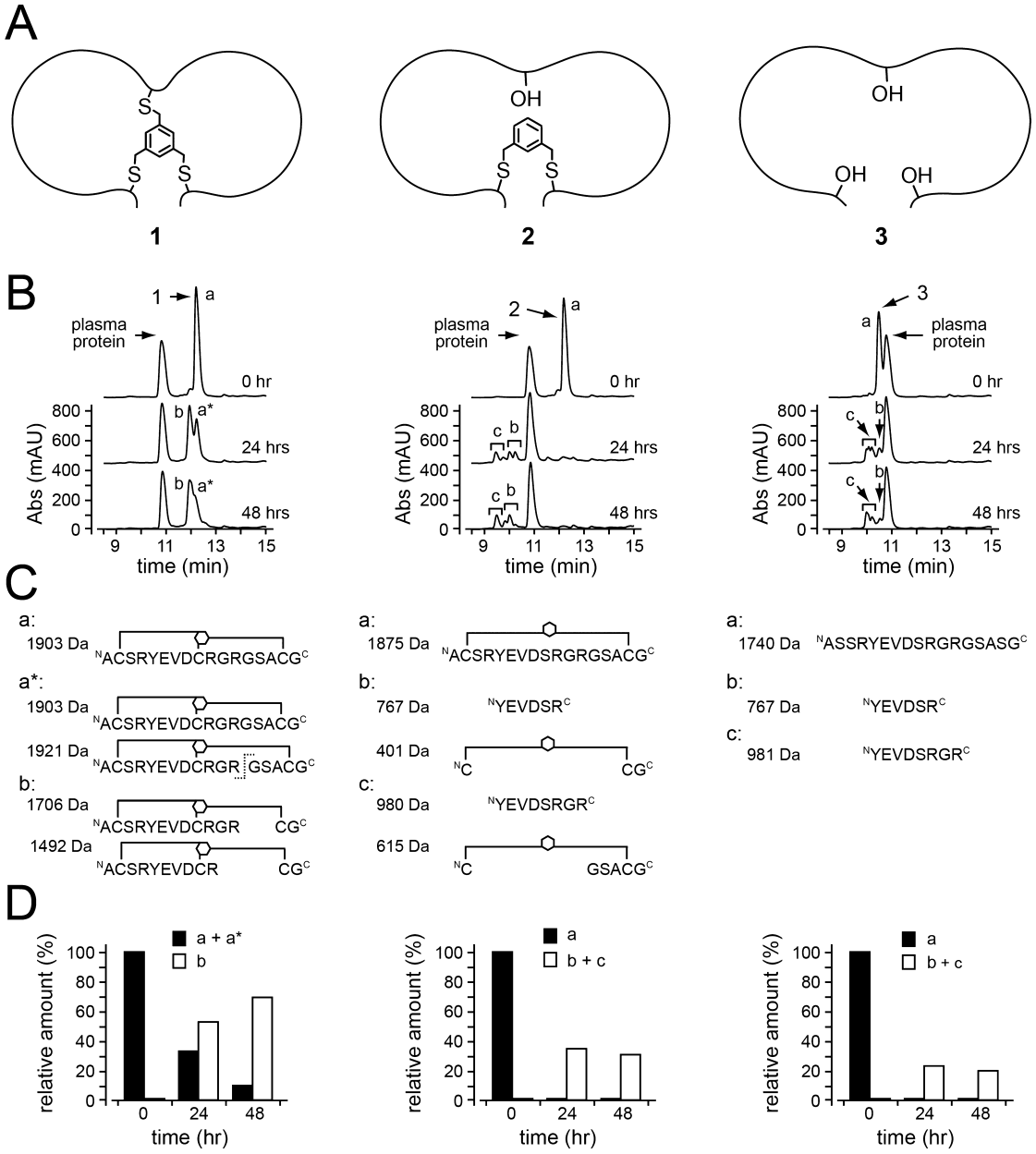

Figure 1. Stability of different peptide formats. (A) Schematic drawing of bicyclic peptide **1**, monocylic peptide **2**, and linear peptide **3**. (B) Chromatographic analysis of peptides incubated in mouse plasma for 0, 24, and 48 h at a concentration of 50 μM and 37 °C. Samples were analyzed by reversed-phase chromatography (RP-HPLC) using a C8 column and absorption measured at a wavelength of 220 nm. (C) Masses of peptides detected by ESI mass spectrometry in the indicated peaks of the RP-HPLC chromatograms. The peptides and peptide fragments that potentially correspond to the masses are schematically depicted. (D) The relative amounts of peptide and peptide fragments were quantified by integrating the peak area in the RP-HPLC chromatograms and are represented in a bar diagram. The relative amount of intact or marginally modified peptide is shown in black, and that of massively degraded peptide is shown in white.

are screened by phage display or other display techniques to isolate binders to numerous targets. More recently, a method based on phage display was developed to generate and screen random bicyclic peptide libraries.[14] Bicyclic peptides are obtained by chemically linking linear peptides of the format Cys-(Xaa)$_n$-Cys-(Xaa)$_n$-Cys (the number of amino acids "n" is typically between 3 and 6) via the three cysteine residues to tris-(bromomethyl)benzene (TBMB).[15] We have applied this approach for the isolation of bicyclic peptide binders to different targets including the urokinase-type plasminogen activator (uPA),[16] a serine protease implicated in tumor growth and invasion.[17] The most potent bicyclic peptide inhibitor **1** (UK18; H-ACSRYEVDCRGRGSACG-NH$_2$; the underlined cysteines are linked to TBMB) blocked human uPA with a K_i of 53 nM and was highly specific. Crystallization of the complex revealed that the bicyclic peptide forms a large interaction surface with uPA (>700 Å^2).[16]

In this work, we aimed at assessing the proteolytic stability of the in vitro-evolved bicyclic peptide inhibitor of uPA and at understanding whether the in vitro-evolved bicyclic peptides are more stable than other peptide formats. Toward this end, we synthesized a range of linear and monocyclic analogues of the bicyclic peptide **1** and compared their stabilities in blood plasma ex vivo. These experiments revealed an unexpected

dx.doi.org/10.1021/jm301276e | J. Med. Chem. 2012, 55, 10187−10197

stabilization mechanism of bicyclic peptides. In the second part of this work, we linked the bicyclic peptide to an albumin-binding tag to enable a longer circulation time, which would be required for the inhibition of uPA for extended time periods. This longer exposure of the bicyclic peptide to serum proteases allowed us to test its stability in vivo for multiple days. Tethering to albumin further increased the stability of the peptide through yet another mechanism and yielded an antagonist that was completely stable in vivo for multiple days.

RESULTS

Plasma Stability of Linear, Monocyclic, and Bicyclic Peptide Formats. The stability of bicyclic peptide **1** (Figure 1A, left) was assessed by incubating the peptide in mouse plasma at a concentration of 50 μM for 24 and 48 h at 37 °C and analyzing the resulting species by chromatography and mass spectrometry (Figure 1B, left). After 24 h, three new species with minor modifications were observed in addition to the intact bicyclic peptide (Figures S1A and S2A in the Supporting Information). After 48 h, a significant quantity of intact bicyclic peptide was still present, whereas the fraction of proteolyzed peptide had slightly increased (Figure 1D, left). In a second experiment, the monocyclic peptide **2** (monocyclic UK18) having only one macrocyclic ring generated by connecting the two terminal cysteines of an analogous peptide (H-ACSRYEVDSRGRGSACG-NH_2)[16] with *m*-di-(bromomethyl)benzene (DBMB) was treated equivalently (Figure 1A, middle). In contrast to the bicyclic structure, the monocyclic peptide was rapidly degraded (Figure 1B, middle). The detectable degradation products were found to be linearized peptides, while around 60% of the peptide was digested into smaller fragments that could not be detected by HPLC (Figure 1C,D, middle, and Figures S1B and S2B in the Supporting Information). Not surprisingly, the linear peptide **3** with a sequence similar to **1** (all three cysteines are replaced by serines: H-ASSRYEVDSRGRGSASG-NH_2) (Figure 1A, right)[16] was rapidly hydrolyzed as well (Figure 1B–D, right, and Figures S1C and S2C in the Supporting Information). In none of the peptide formats was oxidation of the thioether bonds or modification of amino acid side chains observed.

Proteolytic Stability of the Two Individual Rings of a Bicyclic Peptide. Intrigued by the high stability of the bicyclic peptide format, we investigated the mechanism of stabilization. One plausible explanation is that the smaller macrocyclic rings in the bicyclic peptide structure (rings of eight amino acids) are more conformationally constrained than the large ring of the monocyclic peptide format (ring of 15 amino acids) and are therefore less susceptible to proteases. To compare peptides of equal ring size, we synthesized the two peptide rings of **1** individually (Figure 2A). The N-terminal ring **4** (H-ACSRYEVDC-NH_2) (Figures S3A and S3B in the Supporting Information) and the C-terminal ring **5** (H-CRGRGSACG-NH_2) (Figures S3C and S3D in the Supporting Information) were cyclized with DBMB and exposed to mouse plasma. After only 24 h of incubation, both of the peptides could not be detected anymore, and the observed degradation products were heavily modified (Figure 2). Mass spectrometric analysis indicated that the N-terminal ring **4** had lost the exocyclic alanine and peptide fragments within the ring (Figure 2C, left, and Figures S3E and S4A in the Supporting Information). In the C-terminal peptide ring **5**, all amino acids of the peptide loop were excised (Figure 2C, right, and Figures S3F and S4B in the Supporting Information).

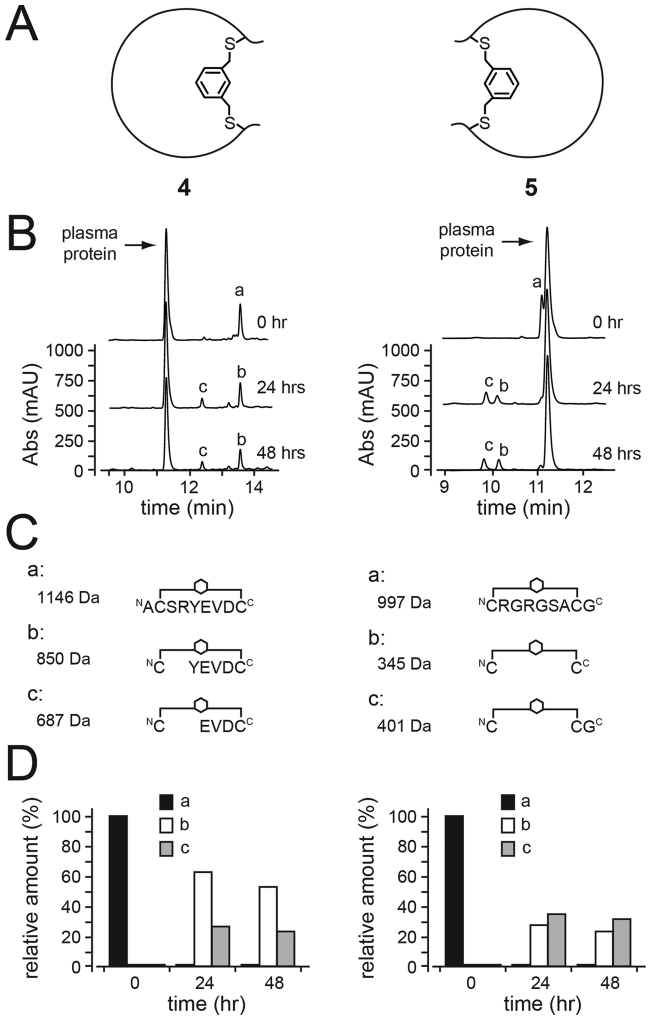

Figure 2. Stability of the two individual peptide rings of **1**. (A) Schematic drawing of the N- and C-terminal peptide rings **4** and **5**. (B) Chromatographic analysis of peptides incubated in mouse plasma for 0, 24, and 48 h at a concentration of 50 μM and 37 °C. Samples were analyzed by reversed-phase chromatography (RP-HPLC) using a C8 column and absorption measured at a wavelength of 220 nm. (C) Masses of peptides detected by ESI mass spectrometry in the indicated peaks of the RP-HPLC chromatograms. The peptides and peptide fragments that potentially correspond to the masses are schematically depicted. (D) The relative amounts of the intact monocyclic peptides and degradation products were quantified by integrating the peak area in the RP-HPLC chromatograms and are represented in a bar diagram. The relative amount of intact cyclic peptide is shown in black, and the different degradation products are shown in gray and white.

Half-Life and Metabolic Stability of Bicyclic Peptide 1 in Vivo. The elimination half-life ($t_{1/2}$) and metabolic stability of **1** were assessed in mice. To facilitate detection and quantification in plasma samples, **1** was synthesized with a fluorescent tag (Figure 3A). Because the C-terminal end of **1** was freely accessible in the uPA/**1** complex as previously determined by X-ray crystallography,[16] fluorescein was linked to this end of the molecule. A linear peptide **6** based on **1** but extended at the C terminus with a Gly-Ser-Gly linker and L-propargylglycine was synthesized, cyclized with TBMB (yielding **7**), and linked to fluorescein-azide by cycloaddition (Figures S5 and S6 in the Supporting Information). This fluorescein-labeled bicyclic peptide **8** (UK18-fluorescein) efficiently inhibited uPA (K_i = 82 nM), indicating that the

dx.doi.org/10.1021/jm301276e | J. Med. Chem. 2012, 55, 10187–10197

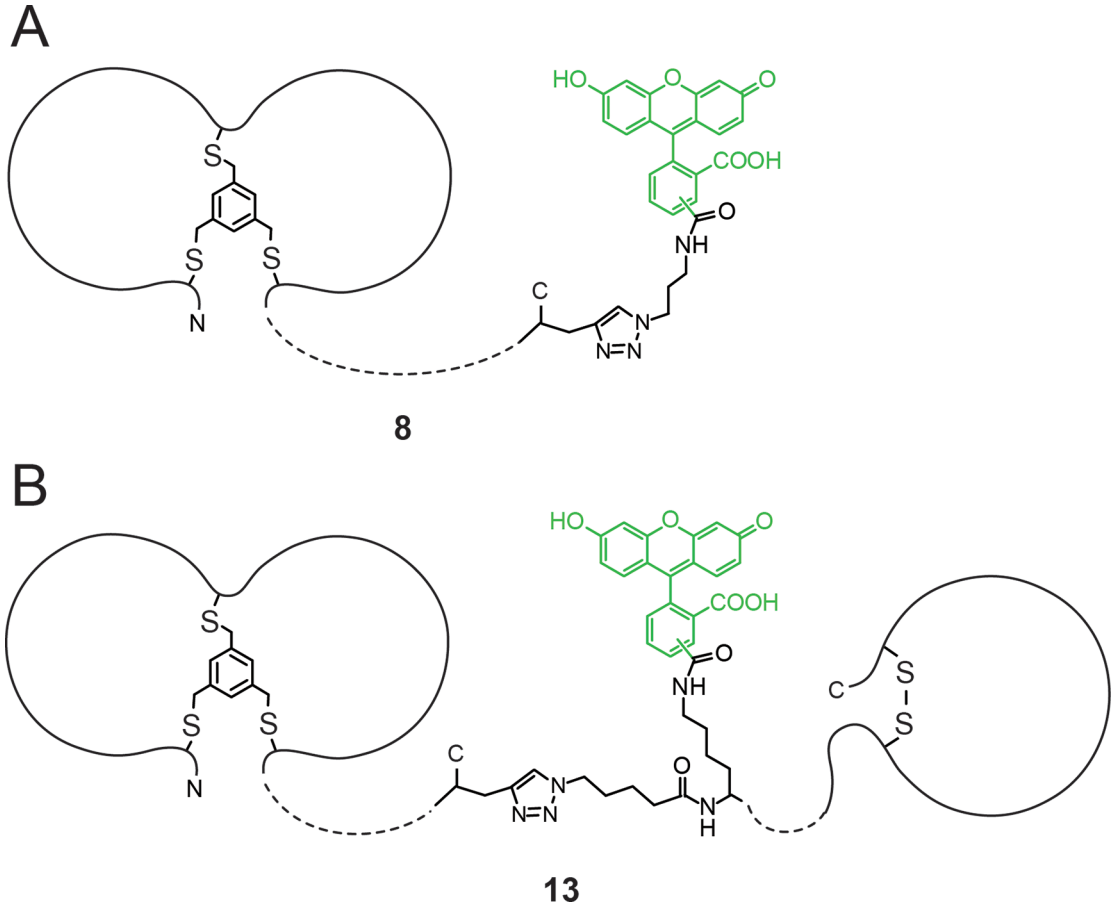

Figure 3. Schematic drawing of **8** (A) and **13** (B). Key chemical structures such as the mesitylene linker in the bicyclic peptide, the disulfide bridge in the albumin binding peptide **9**, the triazole linker, and the fluorescein (highlighted in green) are shown.

linker and fluorescent tag did not significantly affect binding to the protease (Table 1). Two hundred microliters of 50 μM **8** (corresponding to 1.25 mg/kg) was injected intravenously into mice. The concentration of conjugate was quantified at different time points by two complementary assays. Analysis of the samples by reversed-phase ultrafast liquid chromatography (UFLC) gave $t_{1/2}$ α and $t_{1/2}$ β values of 2.9 and 30 min, respectively (Figure 4A and Table 2). The UFLC analysis showed a single fluorescent species in the plasma samples eluting with the same retention time as **8**. In a different assay based on ELISA, **8** was captured by immobilized uPA and detected with an antifluorescein antibody conjugate. This assay gave essentially the same $t_{1/2}$ α and $t_{1/2}$ β values of 2.9 and 29 min, respectively (Figure 4B and Table 2). Elution of **8** as a single peak in the reversed-phase liquid chromatography and binding to uPA in the ELISA assay suggested that most, if not all, of the bicyclic peptide remained intact during the first hour of circulation. Because of the relatively short half-life of the bicyclic peptide, its stability could not be assessed over a longer time period.

Table 1. Inhibition of Human uPA by 1, 8, and 13[a]

	Inhibitory Activity $K_i \pm$ SE (nM)		
	1	**8**	**13**
casein	52 ± 2	82 ± 2	17 ± 1
casein/hSA	60 ± 1	ND	48 ± 2
casein/mSA	54 ± 3	ND	132 ± 9
bSA	53 ± 4	86 ± 4	ND
ovA	56 ± 5	ND	ND

[a]Inhibitory activities (K_i) were determined at 25 °C and physiological pH (7.4) using a chromogenic substrate (H-Glu-Gly-Arg-pNA). The inhibition was tested in the presence of 0.1% (w/v) casein or 0.1% (w/v) casein and either 1.5 μM hSA or 1.5 μM mSA. Additionally, the inhibition was tested in the presence of 0.1% (w/v) ovA or 0.1% (w/v) bSA. The indicated values are means of at least three measurements. SE, standard error.

Extending the Plasma Circulation Time of Bicyclic Peptide 1. We were interested in extending the circulation time of **1** to facilitate future testing of its inhibitory effect on tumor growth in mice. At the same time, a longer half-life would allow measurement of its metabolic stability in vivo over a longer time. The bicyclic peptide **1** was therefore conjugated to the albumin-binding peptide **9** (SA21; Ac-RLIEDI<u>C</u>LPRWG<u>C</u>LWEDD-NH_2; disulfide-cyclized via the underlined cysteine residues), which had been isolated by phage affinity selection against albumin.[18] Previously, conjugation of an antibody Fab fragment to a similar albumin-binding peptide (SA06, H-QRLMEDI<u>C</u>LPRWG<u>C</u>LWEDDF-NH_2) extended its elimination half-life from 1.28 to 19.7 h in mice and from 5.9 to 68.5 h in rabbits.[19] In another work, linkage to a related albumin-binding peptide (SA20, Ac-QRLIEDI<u>C</u>LPRWG<u>C</u>LWEDDF-NH_2) prolonged the elimination half-life of growth hormone and prolactin in mice from 0.49 and 0.84 h to 1.94 and 4.78 h, respectively.[20] We generated the conjugate **13**

dx.doi.org/10.1021/jm301276e | J. Med. Chem. 2012, 55, 10187−10197

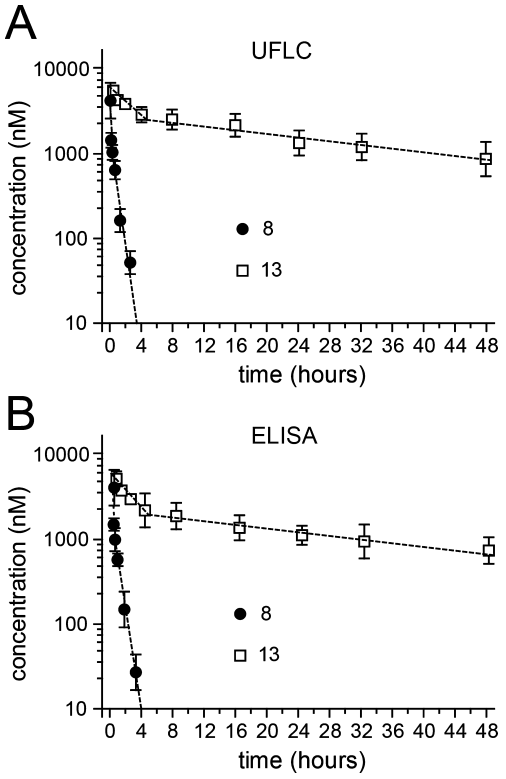

Figure 4. Pharmacokinetic parameters of **8** and **13** in mice. Compounds **8** and **13** were applied intravenously (200 μL of 50 μM; around 25 μg of **8** and 50 μg of **13**), blood samples were taken at the indicated time points, and the concentration of conjugate was measured by reversed-phase UFLC (A) and ELISA (B). The indicated values are averages of at least two mice.

Table 2. Pharmacokinetic Parameters of 8 and 13 in Mice[a]

Pharmacokinetic Parameters	8		13	
	UFLC	ELISA	UFLC	ELISA
C_{max} (μM)	3.98	3.67	5.34	5.16
$t_{1/2}$ α (min)	2.9	2.9	268	229
$t_{1/2}$ β (min)	30	29	1440	1620
$AUC_{0-2days}$ (h μg/mL)	4.7	4.4	964	772
CL (mL/h)	8.78	10	0.089	0.113
V_d (mL)	6.33	6.97	3.09	4.4

[a]Compounds **8** and **13** were applied intravenously (1.25 mg/kg **8** and 2.5 mg/kg **13**), and their concentrations in blood plasma samples were measured by reversed-phase UFLC and ELISA. The maximal concentration (C_{max}) in plasma was measured 5 (for **8**) and 30 min (for **13**) after injection.

(UK18-SA21; Figure 2B) by linking derivatives of the bicyclic peptide **1** and the monocyclic albumin-binding peptide **9** by cycloaddition (Figure S5 in the Supporting Information). The alkyne-functionalized bicyclic peptide **7** was obtained as described above (Figures S5 and S6 in the Supporting Information). The albumin binding peptide derivative **12** was obtained by synthesizing the 18-amino acid peptide **9** (RLIEDICLPRWGCLWEDD) with an N-terminal azido-functionalized Lys-Gly linker (**10**), oxidative cyclization (**11**), and conjugation with NHS-functionalized fluorescein (Figures S5 and S7 in the Supporting Information). In this synthetic strategy, the fluorophore was placed in between **1** and **9** in the conjugate to prevent its loss by N- or C-terminal degradation and to allow tracing of potential fluorescent degradation products (Figure 3B).

The binding of **13** to albumin was assessed by fluorescence polarization. Compound **13** bound to mouse serum albumin (mSA) and human serum albumin (hSA) with K_D values of 14 and 354 nM, respectively (Figure 5A,B and Table 3). Albumin-binding peptide **12** alone (tagged with fluorescein) bound to mSA and hSA with K_D values of 24 and 321 nM, respectively (Table 3 and Figure S8 in the Supporting Information). Fluorescence polarization also allowed measurement of the affinity (K_D) of **13** for human uPA, which was found to be 68 nM (Figure 5C and Table 3).

The inhibitory activities of **1** and conjugates thereof were quantified in activity assays with human uPA and a chromogenic substrate. Compound **13** inhibited uPA more potently (K_i = 17 nM) than either nonconjugated bicyclic peptide **1** (K_i = 53 nM) or **8** (K_i = 82 nM) (Figure 5D and Table 1). The addition of hSA to the assay increased the K_i of **13** to 48 nM (Figure 5D and Table 1), while that of nonconjugated **1** did not change significantly upon hSA addition (K_i = 60 nM) (Table 1). In the presence of mSA, **13** and **1** inhibited human uPA with K_i values of 132 and 54 nM, respectively (Figure 5D and Table 1).

The pharmacokinetic properties of **13** were assessed in mice by intravenous injection (200 μL of a 50 μM solution; corresponding to 2.5 mg/kg) and determination of the concentrations with two different methods. Measurements of the conjugate concentrations by reversed-phase UFLC and fluorescence detection gave $t_{1/2}$ α and $t_{1/2}$ β half-lives of 4.5 and 24 h, respectively (Figure 4A and Table 2). In the chromatographic analysis, only one fluorescent species was observed, suggesting that **13** remained intact. Quantification of the concentrations by sandwich ELISA gave $t_{1/2}$ α and $t_{1/2}$ β half-lives of 3.8 and 27 h, respectively. In this sandwich ELISA, only conjugate with functional bicyclic peptide was detected (Figure 4B and Table 2). The route of elimination of **13** was not investigated, but we expect that most of the conjugate is cleared by the kidney.

Metabolic Stability of Conjugate 13 in Plasma ex Vivo and in Vivo. The stability of **13** in plasma was assessed by incubation in mouse plasma ex vivo for 24 and 48 h at 37 °C, followed by chromatographic and mass spectrometric analysis. For mass spectrometric analysis, the peptide conjugate was first dissociated from albumin by denaturation with 0.1% TFA and successively separated from other serum proteins by reversed-phase liquid chromatography. For direct comparison, the stability of **8** was tested in parallel. Compound **13** eluted in HPLC as a single peak, and mass spectrometric analysis showed a single mass corresponding to the intact conjugate (Figure 6A and Figure S9 in the Supporting Information). In contrast, **8** was eluted in two or three peaks, and mass spectrometric analysis showed a similar extent and pattern of proteolysis as found previously for nontagged bicyclic peptide **1** (Figure S10 in the Supporting Information).

The ELISA assay applied in the pharmacokinetic study suggested that **13** remained functional while in circulation for multiple days, but this assay could not exclude minor modifications such as partial proteolysis or oxidation. We therefore analyzed the mass of **13** in blood samples taken 0, 24, and 48 h postinjection. The fluorescently labeled species were isolated from the mouse plasma samples by reversed-phase UFLC and analyzed by mass spectrometry. A single peak was

dx.doi.org/10.1021/jm301276e | J. Med. Chem. 2012, 55, 10187−10197

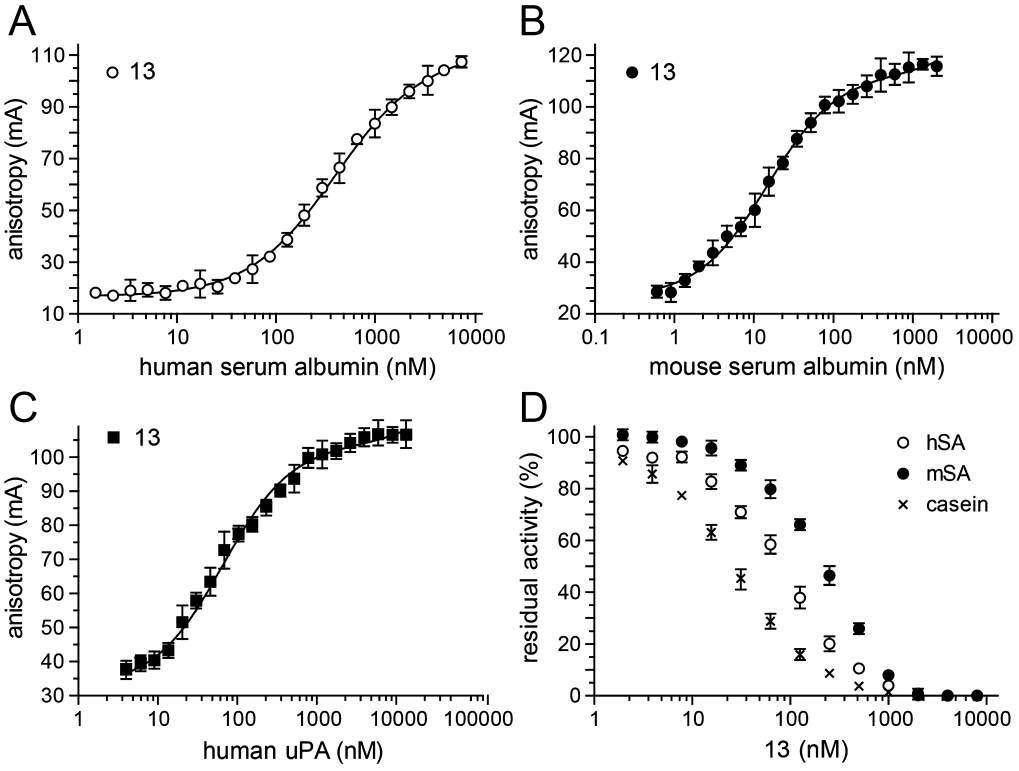

Figure 5. Binding and inhibitory activity of **13**. Binding of **13** to hSA (A), mSA (B), and human uPA (C) was determined by fluorescence polarization. (D) Inhibition of human uPA in the presence of casein only (0.1% w/v) or casein (0.1% w/v) and 1.5 μM hSA or 1.5 μM mSA.

Table 3. Binding Properties of 11 (Albumin-Binding Peptide 9 Tagged with Fluorescein) and 13[a]

	Binding Affinity $K_D \pm$ SE (nM)	
	11	**13**
hSA	321 ± 27	354 ± 19
mSA	24 ± 6	14 ± 3
huPA	ND	68 ± 15

[a]The binding affinity for hSA, mSA, and human uPA was determined by fluorescence polarization (FP) at 25 °C and physiological pH (7.4). The indicated values are means of at least three measurements. SE, standard error.

observed in all three samples, and mass spectrometric analysis showed a single species with a molecular mass of 5097 Da, which corresponded to the intact conjugate (Figure 6B,C).

DISCUSSION AND CONCLUSIONS

In our first set of experiments, we found that an in vitro-evolved bicyclic peptide antagonist possesses high proteolytic stability and is significantly more stable than its monocyclic analogue. Similar observations have been made previously for naturally evolved bicyclic peptides such as sunflower trypsin inhibitor (SFTI-1), a 14-amino acid head-to-tail cyclized peptide with a disulfide bridge that divides the peptide into 29- and 23-membered rings (GRCTKSIPPICFPD).[21,22] Reduction of the Cys3−Cys11 disulfide bond in SFTI-1 was described to lower the stability significantly.[23] At this stage, we assumed that the increased stability of the bicyclic peptides SFTI-1 and **1** resulted primarily from the smaller size of the macrocyclic rings (two 8-aa vs 15-aa in **1** and 7- or 9-aa vs 14-aa in SFTI-1) and the consequent lower conformational flexibility of the peptide backbones.

A second set of experiments showed that the bicyclic peptide **1** is significantly more stable than its two individually synthesized rings. This finding indicated that the bicyclic peptide is not solely stabilized by the increased constraint imposed by the smaller macrocyclic rings and suggested additional stabilization mechanisms. We hypothesize two mechanisms that could explain this stabilization effect. First, the two connected rings may have a lower conformational flexibility due to steric exclusion or noncovalent interactions between the rings, which results in a higher proteolytic stability. Second, one ring may simply shield a region of the second ring from proteolytic attack and vice versa. It is likely that these two mechanisms apply to other bicyclic peptides. In fact, Albericio and co-workers have recently generated bicyclic architectures termed "siamese depsipeptides" by connecting two units of the depsipeptide sansalvamide A by a short linker.[24] Functional characterization of the bicyclic structures suggested a higher conformational constraint, but the effect of bicyclization on the structures' proteolytic stability was not tested.

Chromatographic and mass spectrometric analysis of peptide degradation products yielded information on the extent of proteolysis and hinted at the relevant cleavage sites as well as degradation pathways. The bicyclic peptide was first nicked in one ring, and several amino acids of the opened ring were subsequently degraded. On the basis of the molecular masses, the first cleavage takes place between Arg12 and Gly13. Overall, a significant portion of the bicyclic peptide remained fully intact, and the three degradation products observed after 48 h of incubation in plasma were cleaved at only one of the two rings. In contrast, the monocyclic and linear peptide analogues of **1** were cleaved at multiple sites, resulting in a rapid

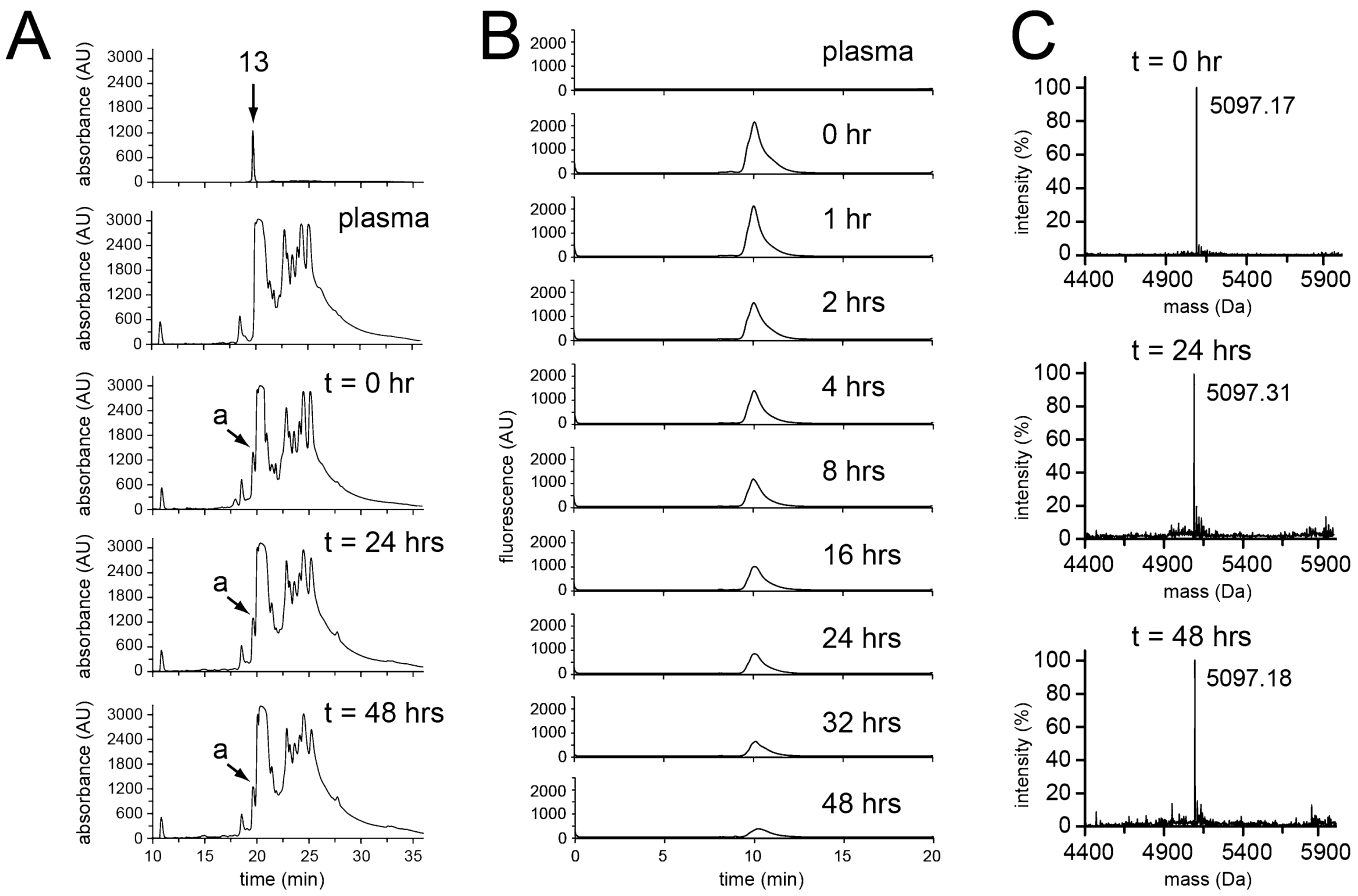

Figure 6. Stability of bicyclic peptide ex vivo and in vivo. (A) Compound **13** incubated in mouse plasma ex vivo was analyzed by reversed-phase chromatography (RP-HPLC) using a C8 column, and absorption was measured at a wavelength of 220 nm. Compound **13** (indicated with "a") eluted immediately prior to a broad peak of multiple plasma components (see also Figure S9 in the Supporting Information). (B) Compound **13** injected into the tail vein of mice, and blood samples were taken after the indicated time points and analyzed by reversed-phase UFLC using a C8 column and fluorescence detection (excitation at 490 nm and emission at 525 nm). Fluorescence monitoring required a buffer system with neutral pH resulting in a broad and asymmetric peak for **13**. Components of plasma did not show fluorescence (first chromatogram). (C) Mass spectra of peaks eluting at between 10 and 11 min in the UFLC chromatogram shown in B. The detected mass corresponded to intact **13** (M_r = 5097 Da).

degradation. Mass spectrometric analysis of the fragments indicated that monocyclic and linear **1** were cleaved at the same preferred sites, after arginine residues in the positions 4 (Arg4), 10 (Arg10), and 12 (Arg12). In the bicyclic peptide, cleavage after Arg4 in the first ring was not observed, and cleavage after Arg10 was slow. In the bicyclic format, these two sites are close to the branching mesitylene group, and access of proteases may be sterically hindered.

Conjugation of **1** to the albumin-binding peptide **9** improved its inhibitory activity by 3-fold, resulting in a K_i of 17 nM. The tighter binding most likely resulted from additional interactions formed between **9** and uPA. In the presence of hSA, the improvement was abrogated, resulting in a K_i of 48 nM, which is close to that of nonconjugated **1** (53 nM). Conjugation of peptides to proteins such as albumin or Fc, or to polymers such as PEG, often reduces their potency by large factors.[25] We were pleased to see that **1** tethered via **9** to albumin retained its activity.

The elimination half-life of **13** was around 50-fold longer than that of **1**. As compared to other peptides or proteins that were tethered via similar peptides to albumin, the elimination half-life of 24 h was surprisingly long. For example, antibody Fab fragment specific for tissue factor fused to SA06 exhibited a half-life of 10.4 h upon intravenous administration to mice.[18] Another Fab fragment specific for Her2 was fused to SA06 and had a half-life of 19.7 h when injected intravenously in mice.[26] The conjugates SA20-hGH and SA20-prolactin applied intraperitoneally to mice had much shorter elimination half-lives of 1.9 and 4.8 h, respectively.[20] These shorter half-lives may have resulted from weaker binding of the conjugates to mSA or from lower metabolic stability. Compound **13** was entirely resistant to proteolysis in mouse plasma ex vivo. Noncovalent tethering of the bicyclic peptide to the surface of albumin appears to shield it from serum proteases. Similar effects were previously described for PEGylated peptides[25] or peptides that were covalently conjugated to serum albumin.[27−30] The clinically approved insulin and GLP-1 tagged with albumin-binding fatty acids demonstrate high stability in vivo and likely also benefit from the same effect.[31,32]

The long half-life of **13** allowed us to further evaluate the stability of the bicyclic peptide in the circulation, where the peptide is additionally exposed to membrane-anchored proteases. Conjugate **13** purified from blood samples taken 2 days postinjection was entirely intact. This result was supported by the finding that reversed-phase UFLC chromatographic analysis of the blood samples showed a single species and that the conjugate was able to bind uPA in a sandwich ELISA even after circulating for 2 days in mice. Low proteolytic stability has hindered the development of long-acting therapeutic peptides. For example, the glucagon-like peptide and variants thereof that

dx.doi.org/10.1021/jm301276e | J. Med. Chem. 2012, 55, 10187−10197

show improved stability are proteolytically degraded by dipeptidyl dipeptidase 4. The albumin-tethered bicyclic peptide **13** clearly overcomes this limitation and paves the way for the development of peptide therapeutics with longer lasting effects.

In summary, we found that an in vitro-evolved bicyclic peptide inhibitor tethered to an albumin-binding peptide is stable for multiple days in vivo. The high stability is likely based on multiple mechanisms, including conformational constraints and shielding effects mediated by the neighboring peptide rings and by albumin. This peptide format overcomes a limitation faced by many in vitro-evolved peptide leads and promises to be suitable for the generation of long-acting peptide therapeutics.

EXPERIMENTAL SECTION

Materials. Fmoc-protected amino acids, Fmoc-rink amide AM resin (0.26 mmol/g resin), *N*,*N*-diisopropylethylamine (DIPEA), and *O*-benzotriazole-*N*,*N*,*N*′,*N*′-tetramethyl-uronium-hexafluoro-phosphate (HBTU) were purchased from Iris Biotech GmbH (Marktredwitz, Germany). Trifluoroacetic acid (TFA), TBMB, *m*-di(bromomehyl)benzene (DBMB), L-ascorbic acid sodium salt, tris((1-benzyl-1*H*-1,2,3-triazol-4-yl)methyl) amine (TBTA), copper(II) sulfate-pentahydrate ($CuSO_4 \cdot H_2O$), tris(2-carboxyethyl)phosphine (TCEP), and 5(6)-carboxyfluorescein *N*-hydroxysuccinimide ester were purchased from Sigma-Aldrich (Steinheim, Germany). 1,2-Ethanedithiol (EDT), thioanisole, and piperidine were obtained from Fluka (Buchs, Switzerland). Phenol was purchased from Acros Organics (Geel, Belgium), 5(6)-carboxyfluorescein azide was from Matabion, 5-azido-pentanoic acid was from Bachem (Bachem, Switzerland), and (*S*)-*N*-Fmoc-propargylglycine was from Shanghai Plus Bio-Sci&Tech (Shanghai, China). All reagents were used as received without further purification. hSA, mSA, bovine serum albumin (bSA), ovalbumin (ovA), and casein were purchased from Sigma-Aldrich. Human uPA was either purchased from Molecular Innovations (Novi, MI) or recombinantly produced and purified in house as previously described.[16]

Peptide Synthesis. Peptides were synthesized on the Advanced ChemTech 348Ω peptide synthesizer (Aapptec, Louisville, United States) by standard Fmoc solid-phase chemistry on a Rink Amide AM resin (0.03 mmol scale) as described previously.[16] The coupling was carried out twice for each amino acid (6 equiv, 0.4 M, in DMF) using HBTU (5.5 equiv, 0.4 M, in DMF) and DIPEA (9 equiv, 1.2 M in DMF). Fmoc groups were removed using a 20% v/v solution of piperidine in DMF. The final peptides were deprotected and cleaved from the resin by treatment with TFA/thioanisole/H_2O/phenol/EDT (90/2.5/2.5/2.5/2.5 v/v, 4 mL) for 3 h at room temperature. The resin was removed by filtration under vacuum, and the peptides were precipitated with cold diethyl ether (40 mL). The precipitated peptides were washed with cold diethyl ether (20 mL × 2). Finally, the peptides were dissolved in H_2O:MeCN (5:2) and lyophilized. Peptides to be cyclized by alkylation were directly treated with TBMB or DBMB without purification (see cyclization protocol below). The linear peptide **3** and the derivatives of **9** were purified by semipreparative reversed-phase HPLC (PrepLC 4000-Waters system, XBridge BEH300 Prep C18 column, 9.4 mm × 250 mm, Waters) using a flow rate of 6 mL/min and a linear gradient of 10−50% v/v solvent B over 30 min (A, 0.1% v/v TFA and 99.9% v/v H_2O; B, 94.9% v/v MeCN, 5% v/v H_2O, and 0.1% v/v TFA). Fractions containing the desired peptide were lyophilized.

Chemical Cyclization. Peptides were cyclized with TBMB as follows. To a solution of crude peptide (8 mL, 0.625 mM peptide) in aqueous buffer (20 mM NH_4HCO_3, pH 8.0), TBMB was added (2 mL, 5 mM in MeCN). The final reagent and solvent concentrations in the reaction mixture were 0.5 mM crude peptide, 1 mM TBMB, 80% v/v aqueous buffer, and 20% v/v MeCN. The reaction mixture was incubated at 30 °C in a water bath for 1 h and then lyophilized. TBMB-modified peptide **1** was purified by semipreparative reversed-phase HPLC as described above. TBMB-modified **7** was purified by size exclusion chromatography using a Superdex Peptide 10/300 GL column (GE Healthcare) and solvent C (30% v/v MeCN, 69.9% v/v H_2O, and 0.1% v/v TFA) on an AKTApurifier system (GE Healthcare). Fractions containing the desired peptide were pooled together and lyophilized.

Peptides were cyclized with DBMB as follows. To a solution of crude peptide (5 mL, 1 mM) in aqueous buffer (20 mM NH_4HCO_3, pH 8.5), DBMB in MeCN (5 mL, 2 mM) was added. The final reagent and solvent concentrations in the reaction mixture were 0.5 mM crude peptide, 1 mM DBMB, 50% v/v aqueous buffer, and 50% v/v MeCN. The reaction mixture was incubated at 37 °C in a water bath for 1 h and then lyophilized. DBMB-modified peptides **2**, **4**, and **6** were purified by semipreparative reversed-phase HPLC as described above and lyophilized.

Peptides were cyclized by disulfide-bridge formation as follows. Air was bubbled for 3 h through a filter-sterilized oxidizing solution of 95% v/v 20 mM NH_4HCO_3 buffer, pH 8.0, and 5% v/v DMSO. The peptide **10** (azido-KG-SA21) (12.7 mg) was dissolved in 20 mL of the oxidizing solution and kept at room temperature for 3 days. After lyophilization, disulfide-cyclized peptide **11** was purified by semipreparative reversed-phase HPLC as described above and the product lyophilized.

Labeling of Peptides with Fluorophores. Fluorescein was conjugated to **7** (bicyclic peptide-GSG-alkyne) as follows (to obtain peptide **8**). In a 1.5 mL eppendorf tube, $CuSO_4 \cdot H_2O$ (100 μL of a 20 mM solution in H_2O mQ) was mixed with TBTA (100 μL of a 20 mM solution in DMSO) and sodium ascorbate (200 μL of a 50 mM solution in H_2O mQ). To the resulting catalytic mixture, a solution of **7** (1.7 mM) and 5(6)-carboxyfluorescein azide (2 mM) in DMSO (0.6 mL) was added. The final reagent and solvent concentrations in the reaction mixture were 1 mM of peptide, 1.2 mM of 5(6)-carboxyfluorescein azide, 2 mM $CuSO_4 \cdot H_2O$, 2 mM TBTA, 10 mM sodium ascorbate, 30% v/v H_2O, and 70% v/v DMSO. The click-chemistry reaction was allowed to proceed at room temperature overnight. The crude reaction was purified by semipreparative reversed-phase HPLC as described above and lyophilized. The mass of **8** was confirmed by ESI-MS (2658.55 Da).

Fluorescein was conjugated to **11** (disulfide-cyclized azido-KG-SA21 peptide) as follows (to obtain peptide **12**). To a solution of **11** (2 mM, 1 equiv) and 5(6)-carboxylfluorescein *N*-hydroxysuccinimide ester (6 mM, 3 equiv) in dry DMSO (0.5 mL), 12.5 μL of DIPEA was added. The reaction mixture was kept at room temperature for 1 h and then purified by semipreparative reversed-phase HPLC as described above. Fractions containing the desired peptide were lyophilized.

Linking Bicyclic Peptide and Albumin-Binding Peptide by Azide−Alkyne Cycloaddition to Obtain Conjugate 13. In a 1.5 mL eppendorf tube, $CuSO_4 \cdot H_2O$ (100 μL of a 20 mM solution in H_2O mQ) was mixed with TBTA (100 μL of 20 mM solution in DMSO) and sodium ascorbate (200 μL of a 50 mM solution in H_2O mQ). To the resulting catalytic mixture, a solution of the alkyne-functionalized peptide **7** (2 mM) and **12** (1.7 mM) in DMSO (0.6 mL) was added. The final reagent and solvent concentrations in the reaction mixture were 1 mM **12**, 1.2 mM **7**, 2 mM $CuSO_4 \cdot H_2O$, 2 mM TBTA, 10 mM sodium ascorbate, 30% v/v pure H_2O mQ, and 70% v/v DMSO. The reaction was allowed to proceed at room temperature overnight. The crude reaction was purified by semipreparative reversed-phase HPLC as described above, and fractions containing the desired peptide were lyophilized. The mass of **13** was confirmed by ESI-MS (5058.19 Da).

Chromatographic and Mass Spectrometric Analysis of Peptides and Peptide Conjugates. The purity of peptides and peptide conjugates was assessed by analytical reversed-phase HPLC (Waters HPLC equipped with Waters 2487 dual λ absorbance detector and with both Waters 600 pump and controller, Waters) using a Vydac C18 (218TP) column (4.6 mm × 250 mm) (Grace & Co.). At a flow rate of 1 mL/min, a linear gradient was applied with a mobile phase composed of eluant A (0.1% v/v TFA solution, 99.9% v/v H_2O) and eluant B (99.9% v/v MeCN and 0.1% v/v TFA). The purity of all peptides or peptide conjugates was >95%. For mass spectrometric analysis, the samples were mixed with 30% v/v MeCN,

70% v/v H_2O, and 0.1% v/v formic acid. The molecular mass of RP-HPLC purified peptides was determined by electrospray ionization mass spectrometry (ESI-MS) performed on a quadrupole time-of-flight mass spectrometer (Q-TOF) Ultima API (Waters, Millford, MA) operated with the standard ESI source in positive mode or by MALDI-TOF performed on an Axima-CFR plus MALDI-TOF mass spectrometer (Axima-CFR plus, Kratos Shimadzu Biotech, Manchester, United Kingdom). α-Cyano-4-hydroxycinnamic acid (α-CHCA) dissolved in 50% v/v MeCN, 49.9% v/v H_2O, and 0.1% v/v TFA was used as a matrix.

Measuring Binding Affinities by Fluorescence Polarization. Proteins were serially diluted (3/2 fold) in phosphate buffer (10 mM Na_2HPO_4, pH 7.4, and 150 mM NaCl). Serially diluted proteins and fluorescent compounds (peptides and fluorescein also diluted in phosphate buffer) were mixed 1:1 (v/v). Seventy-five microliters of each mixture was transferred into a well of a black 96-well half area microplate (Corning, Corning, NY) and incubated at room temperature for 30 min. The fluorescence polarization of each solution was measured in a multiwell plate reader (Envision 2103, PerkinElmer, Waltham, MA) using an excitation filter at 480 nm and an emission filter at 535 nm. The dissociation constants (K_D) were determined by nonlinear regression analyses of A versus $[P]_T$ using eq 1[33]

$$A = A_f + (A_b - A_f) \times \left[\frac{\left([L]_T + K_D + [P]_T - \sqrt{([[L]_T + K_D + [P]_T)^2 - 4[L]_T[P]_T} \right)}{2[L]_T} \right] \quad (1)$$

where A is the experimental fluorescence anisotropy. A_f and A_b are the fluorescence anisotropy for the free and the fully bound fluorescent ligand, respectively. $[L]_T$ and $[P]_T$ represent the total fluorescent ligand and protein concentration, respectively. K_D is the dissociation constant for the binding equilibrium. Values were determined using OriginPro 8G software (OriginLab Corporation), and graphs were made with GraphPad Prism 5.01 software (GraphPad software).

Determination of Inhibitory Activities. Inhibition of human uPA by the different peptide conjugates was measured by incubating different concentrations of each peptide (2-fold dilutions, ranging from 8 μM to 1.95 nM) with 1.5 nM human uPA (UPA-LMW, from human urine, 33 kDa). The enzymatic assays were performed at 25 °C in 150 μL volume of buffer containing 10 mM Tris-Cl, pH 7.4, 150 mM NaCl, 10 mM $MgCl_2$, 1 mM $CaCl_2$, 0.01% v/v Triton-X100, and 5% v/v DMSO and using the chromogenic substrate H-Glu-Gly-Arg-pNA (50 μM; Bachem, Bubendorf, Switzerland). The inhibition assay was performed in the presence of 0.1% (w/v) casein alone or 0.1% (w/v) casein with either 1.5 μM hSA or 1.5 μM mSA. Additionally, the inhibition was tested in the presence of 0.1% (w/v) ovA or 0.1% (w/v) bSA. The initial velocities were monitored as changes in absorbance at 405 nm during 1 h on a microtiter plate reader Spectra MAX 340 (Spectramax absorption plate reader, Molecular Devices, Sunnyvale, CA). Apparent equilibrium constants K_i^{app} values were determined by nonlinear regression analyses of V_i/V_0 versus $[I]_0$ using eq 2

$$V_i/V_0 = 1 - \frac{[E]_0 + [I]_0 + K_i^{app} - \sqrt{([E]_0 + [I]_0 + K_i^{app})^2 - 4[E]_0[I]_0}}{2[E]_0} \quad (2)$$

where V_i and V_o are the reaction velocities in the presence and absence of peptide inhibitor, respectively. $[E]_0$ and $[I]_0$ represent the total enzyme and peptide inhibitor concentration, respectively. K_i^{app} is the apparent inhibition constant in the presence of chromogenic substrate. The final K_i was subsequently determined by correcting for the competitive effect of the substrate $[S]_0$ using eq 3

$$K_i = K_i^{app}/(1 + [S]_0/K_m) \quad (3)$$

where the kinetic constant K_m is the K_m for the hydrolysis of H-Glu-Gly-Arg-pNA catalyzed by huPA, which has been determined by standard Michaelis–Menten equations as described previously.[16] Values were determined using OriginPro 8G software (OriginLab Corporation), and graphs were made with GraphPad Prism 5.01 software (GraphPad software, Inc.).

Pharmacokinetic Studies. All animal studies were carried out according to Swiss regulations under a project license granted by the Service de la consommation et des affaires vétérinaires vaudois. Female BALB/c mice (Charles River, France) aged 7–9 weeks were intravenously injected with 200 μL (50 μM in PBS) of **8** (2–3 mice per time point) or **13** (2–3 mice per time point). Blood samples were collected (5, 10, 20, 40, 80, 160, and 320 min after infection of **8** and 0.5, 1, 2, 4, 8, 16, 24, 32, and 48 h after injection of **13**) into EDTA-treated tubes and kept on ice. Cells were removed from plasma by centrifugation at 2000*g* for 15 min at 4 °C. The supernatants (plasma) were transferred to new tubes and centrifuged again at 6000*g* for 15 min at 4 °C. Plasma samples were aliquoted in small volumes (5–20 μL) and kept at −80 °C until further analysis. Analysis by UFLC was performed as follows. Plasma samples were diluted in ammonium acetate buffer (50 mM, pH 7.5) and analyzed on a Shimadzu UFLC system (UFLCXR) equipped with a fluorescence detector (RF-20A XS, excitation-490 nm, emission-525 nm) and a Vydac C8 (208TP) column (4.6 mm × 250 mm) (Grace & Co.). The linear gradient elution was 0–100% v/v solvent B over 15 min at a flow rate of 1 mL/min (A: ammonium acetate buffer, 50 mM, pH 7.5; B: 100% v/v MeCN). Analysis by ELISA was performed as follows: high capacity binding polystyrene 96-microtiter plates (Nunc-Immuno plate, Denmark) were coated with 5 μg/mL (100 μL/well) of active recombinant human uPA in PBS, pH 7.4, overnight at 4 °C. Wells containing immobilized human uPA were washed twice with PBST (PBS containing 0.05% v/v Tween-20, 350 μL/well) and twice with PBS (350 μL/well). This washing procedure was repeated after each incubation period. The microtiter plates were blocked with 350 μL/well of PBST with 1% w/v casein for 1 h at room temperature. Standard and plasma samples were diluted in PBS buffer containing TCEP (2 mM) and incubated in a thermocycler (Eppendorf-Mastercycler, Hamburg, Germany) at 42 °C for 30 min. Serial dilutions (100 μL/well) of the reduced standards (ranging from 60 to 0.7 nM) and plasma samples were added to the microtiter plate coated with human uPA and incubated at room temperature for 1.5 h. Biotinylated goat polyclonal antifluorescein antibody (Abcam, Cambridge, United States) was used for detection of both **13** and **8** in plasma. Primary antifluorescein antibody, diluted 1:50.000 (100 μL/well) in PBST with 1% w/v casein, was added and incubated at room temperature for 1 h. After washing, Neutravidin coupled to Horse Radish Peroxidase (Invitrogen, Paisley, United Kingdom, 1 mg/mL) diluted 1:2000 (100 μL/well) in PBST with 1% w/v casein was added and incubated at room temperature for 30 min. Plates were developed by adding 100 μL/well of 1-Step Ultra TMB-ELISA (Thermo scientific, Rockford, IL) substrate solution. The enzyme reaction was stopped after 30 min by adding 100 μL/well of 2 M sulfuric acid. Signal intensities were measured at 450 nm in a microtiter plate reader Spectra MAX 340 (Molecular Devices). Values were calculated with GraphPad Prism 5.01 software (GraphPad software). The concentrations versus time data were analyzed using a two-compartment model. The volume of distribution (V_d) was calculated by dividing the applied quantity of **8** (25 μg) and **13** (50 μg) by the extrapolated plasma concentration at time 0 (back-extrapolated from the slope of the elimination phase). The clearance (CL) was calculated by multiplying the elimination rate $[\ln(2)/t_{1/2}\ \beta]$ with the volume of distribution (V_d).

Plasma Stability Assays. Peptide (12.5 μL of 1 mM in 100% v/v filter-sterilized H_2O) was added to 237.5 μL of mouse plasma (final peptide concentration was 50 μM in 250 μL final volume). and the mixture was incubated at 37 °C on a thermo block (Eppendorf-Mastercycler). After 0, 24, and 48 h, 50 μL samples were taken, mixed with 50 μL of filter-sterilized H_2O containing 0.1% v/v TFA, and kept at −20 °C until analysis. The samples (100 μL each) were characterized by analytical reversed-phase high-performance liquid chromatography (RP-HPLC) on an Agilent HPLC system (1260 Infinity) equipped with an autocollector and a Vydac C8 (208TP) column (4.6 mm × 250 mm) (Grace & Co.). The linear gradient elution was 0–100% v/v solvent B over 35 min at a flow rate of 1 mL/

min (A: 95% v/v H_2O, 5% v/v MeCN, and 0.1% v/v TFA; B: 95% v/v MeCN, 5% v/v H_2O, and 0.1% v/v TFA). Fractions containing peptide were lyophilized, resuspended in an aqueous 30% v/v MeCN (0.1% v/v formic acid), and analyzed by using either ESI-MS or MALDI-TOF technique.

■ ASSOCIATED CONTENT

Supporting Information

Supplementary figures showing the synthesis strategies of the peptide conjugates and figures showing experimental data from the peptide binding, inhibition, and stability assays. This material is available free of charge via the Internet at http://pubs.acs.org.

■ AUTHOR INFORMATION

Corresponding Author

*Tel: +41(0)21 693 9350. E-mail: christian.heinis@epfl.ch.

Present Addresses

†David H. Koch Institute for Integrative Cancer Research, Massachusetts Institute of Technology, 77 Massachusetts Avenue, Cambridge, Massachusetts 02139, United States.

‡Department of Chemistry, University of Oxford, OX1 3TA Oxford, United Kingdom.

Author Contributions

Alessandro Angelini and Julia Morales-Sanfrutos have contributed equally.

Notes

The authors declare no competing financial interest.

■ ACKNOWLEDGMENTS

We thank Dr. Laure Menin and Luca Fornelli for their help with mass spectrometry experiments and analysis. We gratefully acknowledge Alice Tzeng for critical reading of this manuscript. Furthermore, we are grateful to Luc Reymond, Moser Simone, Prof. Kai Johnsson, and all of the group members for helpful discussions and technical assistance. The financial contributions from the Swiss National Science Foundation (SNSF Professorship PP00P3_123524/1 to C.H.), the National Competence Center for Biomolecular Imaging (NCCBI; Ph.D. fellowship to P.D.), and the Ministerio de Educacion del Gobierno de Espana (postdoc fellowship to J.M.S.) are gratefully acknowledged.

■ ABBREVIATIONS USED

TBMB, tris-(bromomethyl)benzene; TCEP, tris(2-carboxyethyl)phosphine; uPA, urokinase-type plasminogen activator; bSA, bovine serum albumin; hSA, human serum albumin; mSA, mouse serum albumin; ovA, ovalbumin

■ REFERENCES

(1) Werle, M.; Bernkop-Schnurch, A. Strategies to improve plasma half life time of peptide and protein drugs. *Amino Acids* **2006**, *30*, 351−367.

(2) Pollaro, L.; Diderich, P.; Angelini, A.; Bellotto, S.; Wegner, H.; Heinis, C. Measuring net protease activities in biological samples using selective peptidic inhibitors. *Anal. Biochem.* **2012**, *427*, 18−20.

(3) Kontermann, R. E. Strategies for extended serum half-life of protein therapeutics. *Curr. Opin. Biotechnol.* **2011**, *22*, 868−876.

(4) Mezo, A. R.; McDonnell, K. A.; Low, S. C.; Song, J.; Reidy, T. J.; Lu, Q.; Amari, J. V.; Hoehn, T.; Peters, R. T.; Dumont, J.; Bitonti, A. J. Atrial natriuretic peptide-Fc, ANP-Fc, fusion proteins: semisynthesis, in vitro activity and pharmacokinetics in rats. *Bioconjugate Chem.* **2012**, *23*, 518−526.

(5) Tyndall, J. D.; Nall, T.; Fairlie, D. P. Proteases universally recognize beta strands in their active sites. *Chem. Rev.* **2005**, *105*, 973−999.

(6) Trabi, M.; Craik, D. J. Circular proteins—No end in sight. *Trends Biochem. Sci.* **2002**, *27*, 132−138.

(7) Muttenthaler, M.; Andersson, A.; de Araujo, A. D.; Dekan, Z.; Lewis, R. J.; Alewood, P. F. Modulating oxytocin activity and plasma stability by disulfide bond engineering. *J. Med. Chem.* **2010**, *53*, 8585−8596.

(8) Reissmann, S.; Imhof, D. Development of conformationally restricted analogues of bradykinin and somatostatin using constrained amino acids and different types of cyclization. *Curr. Med. Chem.* **2004**, *11*, 2823−2844.

(9) Bovy, P. R. Structure activity in the atrial natriuretic peptide (ANP) family. *Med. Res. Rev.* **1990**, *10*, 115−142.

(10) Daly, N. L.; Craik, D. J. Bioactive cystine knot proteins. *Curr. Opin. Chem. Biol.* **2011**, *15*, 362−368.

(11) Miljanich, G. P. Ziconotide: Neuronal calcium channel blocker for treating severe chronic pain. *Curr. Med. Chem.* **2004**, *11*, 3029−3040.

(12) Colgrave, M. L.; Craik, D. J. Thermal, chemical, and enzymatic stability of the cyclotide kalata B1: The importance of the cyclic cystine knot. *Biochemistry* **2004**, *43*, 5965−5975.

(13) Melusine. www.melusine.com.

(14) Heinis, C.; Rutherford, T.; Freund, S.; Winter, G. Phage-encoded combinatorial chemical libraries based on bicyclic peptides. *Nat. Chem. Biol.* **2009**, *5*, 502−507.

(15) Timmerman, P.; Beld, J.; Puijk, W. C.; Meloen, R. H. Rapid and quantitative cyclization of multiple peptide loops onto synthetic scaffolds for structural mimicry of protein surfaces. *ChemBioChem* **2005**, *6*, 821−824.

(16) Angelini, A.; Cendron, L.; Chen, S.; Touati, J.; Winter, G.; Zanotti, G.; Heinis, C. Bicyclic peptide inhibitor reveals large contact interface with a protease target. *ACS Chem. Biol.* **2012**, *7*, 817−821.

(17) Andreasen, P. A.; Egelund, R.; Petersen, H. H. The plasminogen activation system in tumor growth, invasion, and metastasis. *Cell. Mol. Life Sci.* **2000**, *57*, 25−40.

(18) Dennis, M. S.; Zhang, M.; Meng, Y. G.; Kadkhodayan, M.; Kirchhofer, D.; Combs, D.; Damico, L. A. Albumin binding as a general strategy for improving the pharmacokinetics of proteins. *J. Biol. Chem.* **2002**, *277*, 35035−35043.

(19) Nguyen, A.; Reyes, A. E., 2nd; Zhang, M.; McDonald, P.; Wong, W. L.; Damico, L. A.; Dennis, M. S. The pharmacokinetics of an albumin-binding Fab (AB.Fab) can be modulated as a function of affinity for albumin. *Protein Eng., Des. Sel.* **2006**, *19*, 291−297.

(20) Langenheim, J. F.; Chen, W. Y. Improving the pharmacokinetics/pharmacodynamics of prolactin, GH, and their antagonists by fusion to a synthetic albumin-binding peptide. *J. Endocrinol.* **2009**, *203*, 375−387.

(21) Korsinczky, M. L.; Schirra, H. J.; Craik, D. J. Sunflower trypsin inhibitor-1. *Curr. Protein Pept. Sci.* **2004**, *5*, 351−364.

(22) Luckett, S.; Garcia, R. S.; Barker, J. J.; Konarev, A. V.; Shewry, P. R.; Clarke, A. R.; Brady, R. L. High-resolution structure of a potent, cyclic proteinase inhibitor from sunflower seeds. *J. Mol. Biol.* **1999**, *290*, 525−533.

(23) Colgrave, M. L.; Korsinczky, M. J.; Clark, R. J.; Foley, F.; Craik, D. J. Sunflower trypsin inhibitor-1, proteolytic studies on a trypsin inhibitor peptide and its analogs. *Biopolymers* **2010**, *94*, 665−672.

(24) Ruiz-Rodriguez, J.; Spengler, J.; Albericio, F. Siamese depsipeptides: constrained bicyclic architectures. *Angew. Chem.* **2009**, *48*, 8564−8567.

(25) Harris, J. M.; Chess, R. B. Effect of pegylation on pharmaceuticals. *Nature Rev. Drug Discovery* **2003**, *2*, 214−221.

(26) Dennis, M. S.; Jin, H.; Dugger, D.; Yang, R.; McFarland, L.; Ogasawara, A.; Williams, S.; Cole, M. J.; Ross, S.; Schwall, R. Imaging tumors with an albumin-binding Fab, a novel tumor-targeting agent. *Cancer Res.* **2007**, *67*, 254−261.

(27) Holmes, D. L.; Thibaudeau, K.; L'Archeveque, B.; Milner, P. G.; Ezrin, A. M.; Bridon, D. P. Site specific 1:1 opioid:albumin conjugate

with in vitro activity and long in vivo duration. *Bioconjugate Chem.* **2000**, *11*, 439−444.
(28) Leger, R.; Benquet, C.; Huang, X.; Quraishi, O.; van Wyk, P.; Bridon, D. Kringle 5 peptide-albumin conjugates with anti-migratory activity. *Bioorg. Med. Chem. Lett.* **2004**, *14*, 841−845.
(29) Leger, R.; Robitaille, M.; Quraishi, O.; Denholm, E.; Benquet, C.; Carette, J.; van Wyk, P.; Pellerin, I.; Bousquet-Gagnon, N.; Castaigne, J. P.; Bridon, D. Synthesis and in vitro analysis of atrial natriuretic peptide-albumin conjugates. *Bioorg. Med. Chem. Lett.* **2003**, *13*, 3571−3575.
(30) Leger, R.; Thibaudeau, K.; Robitaille, M.; Quraishi, O.; van Wyk, P.; Bousquet-Gagnon, N.; Carette, J.; Castaigne, J. P.; Bridon, D. P. Identification of CJC-1131-albumin bioconjugate as a stable and bioactive GLP-1(7−36) analog. *Bioorg. Med. Chem. Lett.* **2004**, *14*, 4395−4398.
(31) Knudsen, L. B. Glucagon-like peptide-1: the basis of a new class of treatment for type 2 diabetes. *J. Med. Chem.* **2004**, *47*, 4128−4134.
(32) Knudsen, L. B.; Nielsen, P. F.; Huusfeldt, P. O.; Johansen, N. L.; Madsen, K.; Pedersen, F. Z.; Thogersen, H.; Wilken, M.; Agerso, H. Potent derivatives of glucagon-like peptide-1 with pharmacokinetic properties suitable for once daily administration. *J. Med. Chem.* **2000**, *43*, 1664−1669.
(33) Roehrl, M. H.; Wang, J. Y.; Wagner, G. A general framework for development and data analysis of competitive high-throughput screens for small-molecule inhibitors of protein-protein interactions by fluorescence polarization. *Biochemistry* **2004**, *43*, 16056−16066.